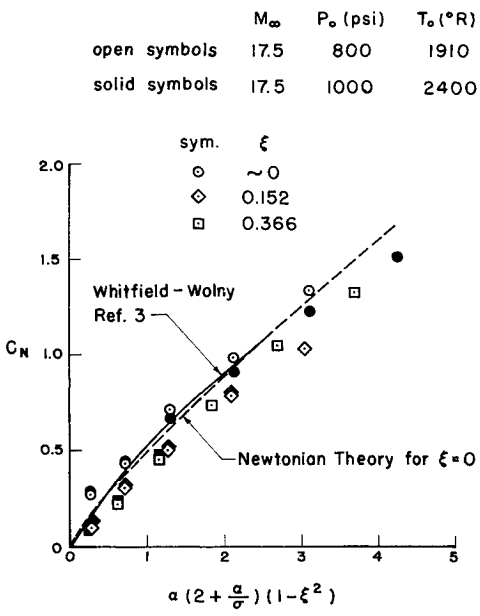

Fig. 3 Correlation of normal force coefficients.

bellows of 0.062 in. o.d. × 0.040 in. i.d. × 0.0003 in. wall thickness. Screw threads at the base of the balance allow the attachment of interchangeable models.

The axial section of the balance has three flexures. The foil strain-gages are mounted on the center flexure to reduce the pitch-on-drag interaction. The pitch sections are of the eccentrically loaded column type with the forward and the aft gages spaced longitudinally about 0.5 in. apart. An iron-constantan thermocouple is mounted on the axial section so that the effect of balance temperature on balance response can be accounted for.

Tests indicate that the balance can measure forces from 0.001 lb to 0.06 lb with an accuracy of ±0.0002 lb. A detailed description of the balance is given in Ref. 1.

3. Test Results Obtained with Cone Models

Tests were made with 10° cones of tip bluntness ratios ξ up to 0.366 (see Fig. 2 for cone geometry and nomenclature).

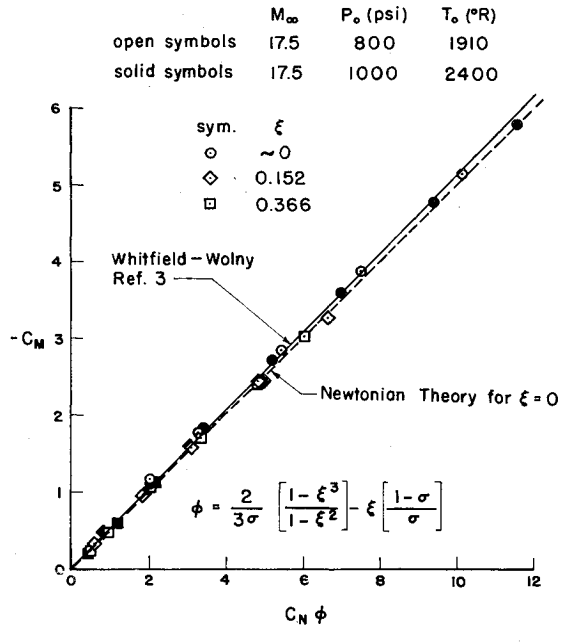

Fig. 4 Correlation of pitching moment coefficients.

The cones all have a base diameter of 0.656 in. and are 3.75 in. long when measured from the vertex. A series of force measurements has been carried out with angles of attack varying from 0° to 30°. These tests were performed in NOL Hypersonic Tunnel 4 that uses nitrogen heated by a graphite resistance heater as the test gas.[2] The gas is expanded to a test Mach number of 17.5 through a $9\frac{1}{2}°$ conical nozzle. The Reynolds number based on the length of the cones is about 25,000.

In Figs. 3 and 4 the normal force and pitching moment coefficients are correlated in terms of the parameters suggested by Whitfield and Wolny.[3] The pitching moment is defined as the moment about the nose (stagnation point at $\alpha = 0°$). The wall temperature of the cones was about 700°R for all the test results.

Since the tests were mainly for the purpose of checking out the balance, they were run at rather low supply temperatures of 1900 to 2400°R in order to extend the lifetime of the graphite resistance heater. At these temperatures the theoretical static temperature in the test section was below the condensation threshold, but no difficulties with condensation appeared to be present in the experimental results. Tests with higher supply temperatures will be reported on later.

References

[1] Horanoff, E. V., "Design of a miniature, water-cooled, internal strain-gage wind tunnel balance," Naval Ordnance Laboratory NOLTR 64-136 (to be published).

[2] Harris, E. L., Carner, J. W., Pasiuk, L., and Wint, C. T., "NOL Mach 17 nitrogen wind tunnel," Naval Ordnance Laboratory NOLTR 64-128 (September 1964).

[3] Whitfield, J. D. and Wolny, W., "Hypersonic static stability of blunt slender cones," Arnold Engineering Development Center AEDC-TDR-62-166 (August 1962).

Sensitivity of Flow Visualization Methods at Low-Density Flow Conditions

W. F. Merzkirch*
NASA Ames Research Center, Moffett Field, Calif.

THE advantages of direct flow visualization methods using schlieren and interferometer techniques are obvious, provided that the differences in flow density to be visualized are large enough. Since the latter condition may not be fulfilled in some low-density hypersonic flows, sensitivity limits of optical methods for visualizing weak shock waves at low gas density conditions have been investigated (e.g., Refs. 1 and 2). Reference 2 also contains theoretical considerations for the schlieren-interferometer system. The experimental results, however, may be restricted by the quality of the respective optical systems. In this note an attempt is made to analyze theoretically the sensitivity limits for two interferometer systems and the schlieren method.

First of all, the fundamental difference between the interferometer and the schlieren methods has to be emphasized. The first method is sensitive to absolute differences in gas density, whereas the latter is sensitive to density gradients. This restricts the general validity of the results given in Refs. 1 and 2. The interferometer is capable of visualizing an ideal shock of zero thickness, whereas the schlieren method cannot detect an ideal shock with infinite density gradient. The visualization of a shock wave with the schlieren method is

Received December 23, 1964.

* Postdoctoral Research Associate, National Academy of Sciences. Member AIAA.

possible since the shock has a finite thickness that increases with decreasing density or Reynolds number. For a more general analysis, the effect of the shock thickness or the real density distribution in the shock wave must be included in investigations of sensitivity.

In the schlieren-interferometer system, a primary light ray is separated by a Wollaston prism into two polarized rays passing through the test section with a small distance d between them. In the test section they pass through regions of different gas density. Behind a second prism the two rays are recombined and can interfere on the film plane. The relative shift of interference fringes $\Delta S/S$, where S is the fringe width for an undisturbed field of view, is related to the density difference $\Delta\rho$ by a formula given by Oertel[3]:

$$\Delta S/S = (Z/\lambda)\cdot K\cdot\Delta\rho \tag{1}$$

where Z is the length of the path travelled by the disturbed ray that, in practice, is the width of the test section or the width of a two-dimensional model, λ is the light wavelength, and K is a constant given by the Gladstone-Dale formula. For air, $K = 0.227$ cm^3/g. With the assumption that a relative fringe shift of 5% is distinguishable, that is, $\Delta S/S = 0.05$, $\lambda = 0.5\mu$, and $Z = 10$ cm, the smallest density difference that can be visualized with air as test gas is

$$\Delta\rho \approx 1 \times 10^{-6}\ \text{g/cm}^3$$

This is the density difference that has to exist between the two separated rays in the test section and can result in the visualization of an ideal shock.

Equation (1) also applies to the Mach-Zehnder interferometer, although the form of the fringe shift is somewhat different from the case of the schlieren interferometer (see, e.g., the interferograms of Ref. 1) Also the condition relating the density difference $\Delta\rho$ to the small distance d between the separated rays does not apply here, but for the visualization of an ideal shock, both interferometers have the same sensitivity.

An analysis of the schlieren system is more complicated. According to Schardin,[4] an expression for its sensitivity is given by the intensity ratio $\Delta E/E$, where E is the intensity in the film plane for an undisturbed field of view and ΔE is the intensity change there caused by a light deflection of an angle ϵ in the test section. For a schlieren system with parallel light through the test section, the test section adjacent to a lens or mirror of focal length f and the knife-edge in the focal point of the mirror, Schardin derives

$$\Delta E/E = (f/a)\epsilon \tag{2}$$

where a is the portion of the light that passes over the knife-edge in the undisturbed case. (For a double-pass system, f is replaced by the radius of curvature $R = 2f$ of the mirror.)

The ratio $\Delta E/E$ can be increased by reducing the aperture a of the knife-edge. Apart from the restrictions that a minimum intensity is required for exposure and that deflections in both directions are to be visualized, there is another important limit in reducing the value of a, and that is determined by light diffraction. For the width u_d that the image of the light source is out of focus, diffraction theory yields

$$u_d = (\lambda/d)f \tag{3}$$

where d is the diameter of the disturbed region, for example, the boundary-layer thickness or shock thickness. According to Schardin one might allow a width $u_d = a$ for the image of the discontinuity being out of focus. Together with Eq. (2) this yields a minimum deflection angle ϵ_d that can be visualized for a given combination of λ, d, and $\Delta E/E$:

$$\epsilon_d = (\Delta E/E)\cdot(\lambda/d) \tag{4}$$

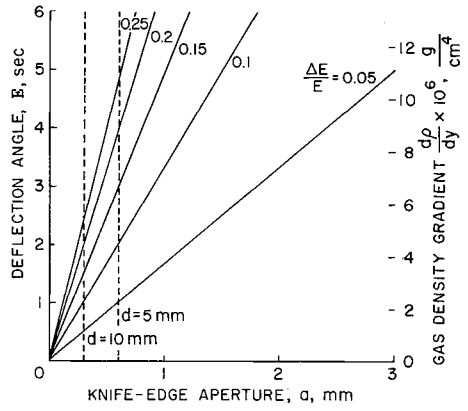

Fig. 1 Deflection angle ϵ and gas density gradient $d\rho/dy$ when the knife-edge aperture a is varied (for $f = 6$ m).

This diffraction limit results in an intensity distribution that is quantitatively related to the density distribution in the test section. For qualitative visualization only, however, one can allow considerably larger values of u_d.

The deflection angle ϵ that can be visualized by varying the aperture a is shown in Fig. 1 for different values of $\Delta E/E$ assuming a focal length $f = 6$ m. One assumes that an intensity change of less than 5% cannot be distinguished; the curve $\Delta E/E = 0.05$ is one limit for visualization. A second limit is the diffraction limit given in Fig. 1 for two values of d. From Fig. 1 it is seen that the smallest deflection angle that can be visualized, with the assumption of a diameter $d = 5$ mm for the disturbed region, is $\epsilon = 1$ sec. If an intensity change of at least 10% is required, this angle becomes $\epsilon = 2$ sec.

The deflection angle ϵ is related to the gradient of the gas density in the test section. For a two-dimensional model and a density change vertical to the knife-edge in the y direction,

$$\epsilon = Z\cdot K\cdot(d\rho/dy) \tag{5}$$

where Z is the model width and K the constant from the Gladstone-Dale formula. In Fig. 1, the observable density gradient is shown for $Z = 10$ cm and air as the test gas ($K = 0.227$ cm^3/g).

This brief analysis shows that a comparison between the interferometer and the schlieren methods can be specified only for a special case of flow conditions, in particular, for a given density distribution. The sensitivity limits described here are of the same order as those experimentally demonstrated in Refs. 1 and 2, and represent maximum values with any imperfection of lenses, mirrors, or other parts of the optical systems neglected.

References

[1] North, R. J. and Stuart, C. M., "Flow visualization and high-speed photography in hypersonic aerodynamics," *Proceedings of the Sixth International Congress on High Speed Photography* (H. D. Tjeenk Willink and Zoon N. V., Haarlem, Holland, 1963), pp. 470–477.

[2] Philbert, M., "Visualisation des écoulements a basse pression," Rech. Aeronaut. **99**, 39–48 (March-April 1964).

[3] Oertel, H., "Visualisierung kurzzeitiger Hyperschallströmungen mit Hilfe eines Differential-Interferometers grosser Öffnung," *Proceedings of the Sixth International Congress on High Speed Photography* (H. D. Tjeenk Willink and Zoon N. V., Haarlem, Holland, 1963), p. 478.

[4] Schardin, H., "Die Schlierenverfahren und ihre Anwendungen," Ergeb. Exakt. Naturw. **20**, 303–439 (1942).